Methodological improvement on local Gabor face recognition based on feature selection and enhanced Borda count

Claudio A. Perez *, Leonardo A. Cament, Luis E. Castillo

Image Processing Laboratory, Department of Electrical Engineering and Advanced Mining Technology Center, Universidad de Chile, Av. Tupper 2007, Santiago, Chile

ARTICLE INFO

ABSTRACT

Face recognition has a wide range of possible applications in surveillance, human computer interfaces and marketing and advertising goods for selected customers according to age and gender. Because of the high classification rate and reduced computational time, one of the best methods for face recognition is based on Gabor jet feature extraction and Borda count classification. In this paper, we propose methodological improvements to increase face recognition rate by selection of Gabor jets using entropy and genetic algorithms. This selection of jets additionally allows faster processing for real-time face recognition. We also propose improvements in the Borda count classification through a weighted Borda count and a threshold to eliminate low score jets from the voting process to increase the face recognition rate. Combinations of Gabor jet selection and Borda count improvements are also proposed. We compare our results with those published in the literature to date and find significant improvements. Our best results on the FERET database are 99.8%, 99.5%, 89.2% and 86.8% recognition rates on the subsets Fb, Fc, Dup1 and Dup2, respectively. Compared to the best results published in the literature, the total number of recognition errors decreased from 163 to 112 (31%). We also tested the proposed method under illumination changes, occlusions with sunglasses and scarves and for small pose variations. Results on two different face databases (AR and Extended Yale B) with significant illumination changes showed over 90% recognition rate. The combination EJS–BTH–BIP reached 98% and 99% recognition rate in images with sunglasses and scarves from the AR database, respectively. The proposed method reached 93.5% recognition on faces with small pose variation of 25° rotation and 98.5% with 15% rotation in the FERET database.

1. Introduction

In most large cities across the world, tens of thousands of cameras have been installed for video surveillance. In the London (UK) subway system, there are over 13,000 cameras installed for surveillance [1]. In Paris (France) there are more than 9500 [2], in Madrid (Spain) more than 6000 [3] and in Santiago (Chile) over 800 cameras [4]. Most metropolitan areas have thousands of cameras installed for surveillance on highways, in malls, department stores, airports, train stations, university campuses, schools and down-town districts streets. In contrast to the massive deployment of cameras, there is very limited capability for monitoring in real time the captured images.

Face recognition technology shows advantages over other biometric identification techniques in specific applications such as "watch list". Face recognition does not require active participation of the subjects and it can be performed at a distance [5]. Additionally, face recognition is possible in cases where the only

information available from a person is a picture. Another advantage of face recognition is that everybody can be enrolled in contrast to fingerprint identification in which a segment of the population does not have a fingerprint compatible with biometric identification [6]. Face recognition is also being developed for selective marketing applications as well as human machine interfaces [7].

Face recognition is a topic of active research and several methods have been proposed to perform this task. Many methods have focused on face and eye localization which are crucial steps previous to face recognition [8–11]. An important number of papers have focused directly on face recognition with the assumption that the face has already been localized [12,13]. We will focus our literature review on the latter methods that have yielded the highest face recognition performance. Eigenfaces [14], based on principal component analysis (PCA), is a method that reduces face image dimensionality by a linear projection that maximizes the dispersion among the projected samples. Fisherfaces [15], based on linear discriminant analysis (LDA), is similar to eigenfaces but uses a linear projection to maximize distance among different classes and minimize distance within each class. Other methods for face recognition are based on the discrete cosine transform (DCT) [16,17] and the Walsh–Hadamard transform (WHT) [18]. The first

---

method compares DCT-based feature vectors from the input and gallery images and the second one is a low complexity algorithm that compares WHT-based feature vectors using mean square error (MSE). Locally linear discriminant embedding (LLDE) [19] improves the locally linear embedding (LLE) method by adding invariance to scale and translation using a class translation vector. The purpose of LLE [20,21] is to map a high dimensional vector into a low dimensional one. Another face recognition method is spectral feature analysis (SFA) [22] which preserves the data's nonlinear manifold structure. SFA is a special case of weighted kernel principal component analysis (KPCA) [23]. Dynamic Training Multistage Clustering (DTMC) [24] is a face recognition method that uses a discriminant analysis to project the face classes and does clustering to divide the projected data. To create the most useful clusters, an entropy-based measure is used. In [25] a Hausdorff distance-based measure is used to represent the gray values of pixels in face images as vectors. It was found that the transformation of the image is less sensitive to illumination variations and also maintains the appearance of the original gray image.

Recently, local matching methods and face representations have become popular in face recognition research. The local binary pattern (LBP) method was proposed in [26], in which the face image is divided into square windows where a binary code is generated whenever a pixel exceeds the value of the average within the window. The distance measure with best results was χ^2, with 97% success rate in Fb FERET set [27]. Gabor wavelets [28–31] have been used to extract local features achieving outstanding results in face recognition. In [32,33] a Sparse representation method is used for face recognition. This method is robust to occlusions, noise, illumination changes and varying pose. Another important aspect of this method is that no information is lost as in methods based on feature extraction.

One of the first methods based on Gabor wavelets for face recognition was the Elastic Bunch Graph Matching (EBGM) method [34]. The EBGM method uses a set of Gabor jets associated to nodes that extract a local feature from the face. EBGM reaches 95% accuracy on the FERET Fb set [27]. Gabor Fisher Classifier (GFC) [35] is a face recognition method that uses the enhanced Fisher linear discriminant model (EFM) [36] on a vector obtained from Gabor representations of images. Local Gabor binary pattern (LGBP) operator is a combination between Gabor wavelets and the LBP operator. Local Gabor binary pattern histogram sequence (LGBPHS) [37] uses the LGBP operator. LGBP maps are obtained for 40 Gabor filters (five scales and eight orientations) on the face image by dividing the image in non-overlapping rectangular windows. A sequence of histograms is computed in each rectangular window and this sequence is compared to the one in the gallery using histogram intersection and weighted histogram intersection [37]. The best results are 98% and 97% for Fb and Fc sets of FERET [37].

A method based on the histogram of Gabor phase patterns (HGPP) [38] uses the phase from the Gabor filter feature to compute the global Gabor phase patterns (GGPP) and local Gabor phase patterns (LGPP) with global and local information about the pixel and vicinity. Similarly to LGBPHS, the image is divided into non-overlapping rectangles and the features are compared using the method of histogram intersection and weighted histogram intersection trained with Fisher separation criterion. The results obtained were 97.5%, 99.5%, 79.5% and 77.8% in Fb, Fc, Dup1 and Dup2 sets of the FERET database [38]. Gabor filters are also employed in a method called local Gabor textons (LGT) [39] where the image is divided into regions generating a cluster for each region based on the Gabor features forming a vocabulary of textons. The vocabulary histogram is compared to those of the gallery using χ^2 with the Fisher criterion weights. The best result of LGT is 97% for the Fb set of FERET database [39].

The face recognition method called learned local Gabor pattern (LLGP) [40] has a learning stage where each training image is filtered by C Gabor filters at different scales and orientations. With the C Gabor features a clustering is performed to generate C codebooks. In the recognition stage the LLGP codebooks are applied to the C Gabor features obtaining C LLGP maps. These maps are divided into non-overlapping regions obtaining a histogram for each region generating a sequence of histograms. This sequence is compared to the histogram intersection and the final classification is performed using the nearest neighbor method. The LLGP method reached 99% in Fa, 99% in Fb, 80% in Dup1 and 78% in Dup2 of the FERET database [40].

The Local Gabor Binary Pattern Whitening PCA (LGBPWP) [41] method is based on LGBPHS and doing the Whitening Process with PCA. This is an improvement over PCA because component discrimination is not lost at high frequencies. Furthermore, this method selects features based on the variance and obtains some of the best published results on the FERET face database in the subsets Dup1, 83.8% and in Dup2, 81.8%, respectively.

An interesting algorithm using 3D and 2D models with Gabor features was proposed in [42]. The enrollment is performed with a 3D model, and then the recognition is done with 2D feature extraction, in which Gabor Filters are used with 3 scales and 8 orientations.

The best results for face recognition published to date in the literature with the FERET face database use the local matching Gabor method (LMG) [43]. The recognition rates were 99.5%, 99.5%, 85.0% and 79.5% for the subsets Fb, Fc, Dup1 and Dup2, respectively. With this method, a total of 4172 Gabor jets are employed to extract features at five different spatial resolutions (λ). A Borda count method is used to compare the inner product among the Gabor jets [43,44] between the input face image and the Gabor jets from faces in the gallery.

In [45], Gabor feature selection is performed with different methods including genetic algorithms (GA) [46,47]. Using this GA method, the 15 most relevant coordinates for Gabor features are selected and the fitness function is the recognition performance.

In a recently published review of Gabor wavelet methods for face recognition [48], research based on Gabor Wavelets is presented, compared and ranked. The method with highest overall performance is LMG [43].

In this paper, we propose several improvements to the LMG method [43] based on Gabor jets selection and Borda count enhancement. The LMG Borda count method was previously compared to another method that combines characteristics using vector/histogram concatenation on the face recognition problem [43]. The best results were obtained with Borda count tested on the FERET database [27]. Additionally, in the Borda count method, each Gabor jet is considered as a feature vector that is compared to the corresponding Gabor jet from the gallery using the cosine distance as a similitude measurement. As in the case of Adaboost [49,50], each Gabor jet constitutes a weak classifier and a large quantity of them are combined in the Borda count method to become a strong classifier [44,43]. We also consider a modification in the Borda count computation by using weights in the input scores.

We propose modifications in the Borda count classifier [43], Gabor jets selection using entropy and GAs, and weighted combination of jets into the Borda count. Besides improving face recognition results, Gabor jet selection allows faster processing for real-time face recognition. We also propose improvements in the Borda count through a weighted Borda count and a threshold for voting to increase the face recognition rate. Combinations of Gabor jet selection and Borda count improvements are also studied. The proposed new method achieves significantly better results than those published in the literature to date. Our results are compared to those of nine recently published papers.

2. Methodology

2.1. Local matching Gabor for face recognition

Face recognition based on local matching Gabor consists of three main modules [43]: image normalization, feature extraction through Gabor jets computation and classification using Borda count matching, as shown in Fig. 1. The first module performs face normalization through image rotation, displacement, and resizing to locate the eyes at a fixed position. The normalized image has the eyes fixed at positions $(67, 125)$ and $(135, 125)$ within a 203×251 pixels image [43]. The second module performs the Gabor jet computation to extract features from the face using the eyes as reference points. Gabor jets are computed on selected points using five grids placed over the face as shown in Fig. 2(a)–(e). The five grids indicate the positions where features are extracted by the Gabor jets at five different spatial resolutions. In correspondence to the grid size, the Gabor wavelet has five spatial scales $0 \leq v \leq 4$ in

$$\psi_{v,\mu} = \frac{\|\vec{k}\|^2}{\sigma^2} \exp\left(-\frac{\|\vec{k}\|^2 \|\vec{r}\|^2}{2\sigma^2}\right) \exp(i\,\vec{k} \cdot \vec{r}), \quad \overline{\psi}_{v,\mu} = \frac{|\psi_{v,\mu}|}{\sqrt{\Sigma_{\mu'=0}^{7} |\psi_{v,\mu}|^2}},$$
(1)

where vectors $\vec{r} = \begin{pmatrix} x \\ y \end{pmatrix}$ and $\vec{k} = \left(\frac{\pi}{2f^v}\right) \begin{pmatrix} \cos\mu\pi/8 \\ \sin\mu\pi/8 \end{pmatrix}$, and constants $f = \sqrt{2}$ and $\sigma = 2\pi$ [31]. The Gabor feature $\overline{\psi}_{v,\mu}$ for $0 \leq \mu \leq 7$ is the unit vector used for jet computation. The spatial scale is equivalent to $\lambda \in \{4, 4\sqrt{2}, 8, 8\sqrt{2}, 16\}$ in pixels [43].

At each point on the grid, the Gabor wavelet has eight different orientations $0 \leq \mu \leq 7$ in (1). Fig. 2(a)–(e) shows with a + sign the position where the Gabor jets are computed and also shows a white square depicting the Gabor jet size for each of the 5 spatial

frequencies. One jet is a set of Gabor features, for the eight orientations, extracted at one point on the grid. Therefore, a jet can be represented by a vector of length 8 for the coordinate (v, x, y). The method assumes that a gallery is available with the faces of the persons to be identified. For each face in the gallery, the Gabor jets are computed off-line and stored in a database for later online recognition. The third module, the Borda count matching, performs a comparison between the set of Gabor jets computed on the input face image and each set of Gabor jets stored in the gallery. This comparison is performed using an inner product between each Gabor jet, which is a vector of length eight at each point of the five grids. The result of the inner product between Gabor jets of the input face image and the Gabor jets of the gallery is a matrix of $N \times M$ dimensions, where N is the number of face images in the gallery and M is the number of jets. The final classification is performed using the Borda count method [44] which selects according to a vote among all jets, the identified face from the gallery. In the Borda count method, all jets are sorted based on inner product results with the gallery elements. The top ranked jet gets the score $N-1$ and the last jet gets score 0. Fig. 3(a) illustrates the Borda count process for a matrix S with dimensions $N \times M$, where S_{ij} is the score of the jth Gabor jet comparison with the ith image of the gallery. Each column C of matrix S is sorted out thus obtaining the matrix with sorted columns O with dimension $N \times M$ as shown in Fig. 3(b). Each component O_{ij} in one column of O is the score from $N-1$ to 0. Finally the complete score for the ith gallery element is the sum of all rows in the ith column of O, and the final score $P_i = \Sigma_{j=1}^{M} O_{ij}$, as shown in Fig. 3(c).

Table 1 shows an example of the Borda count computation score for the case of 6 jets and a gallery with 4 images. The gallery image i_3 obtains the highest score for most of the jets and the highest final score. Face identification is performed choosing the rank-1 image score, i.e., the largest score value is selected as the recognized face, in the P vector.
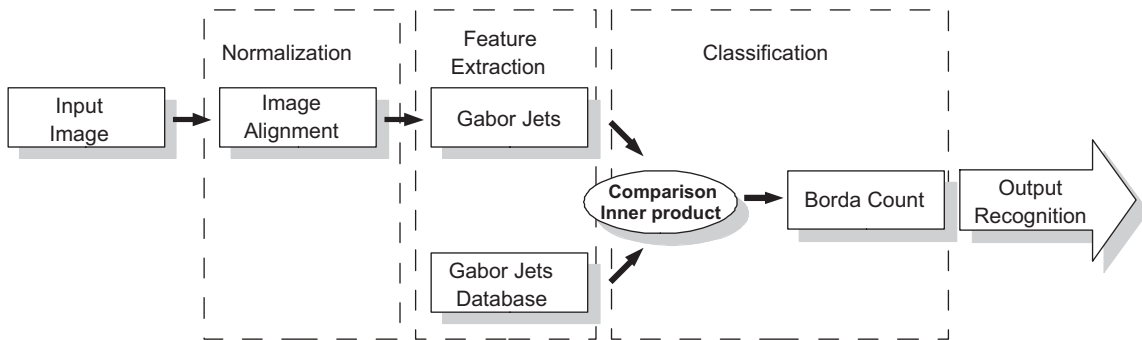

Fig. 1. Local matching Gabor consists of three main modules: image normalization, feature extraction through Gabor jets computation and classification using Borda count matching.

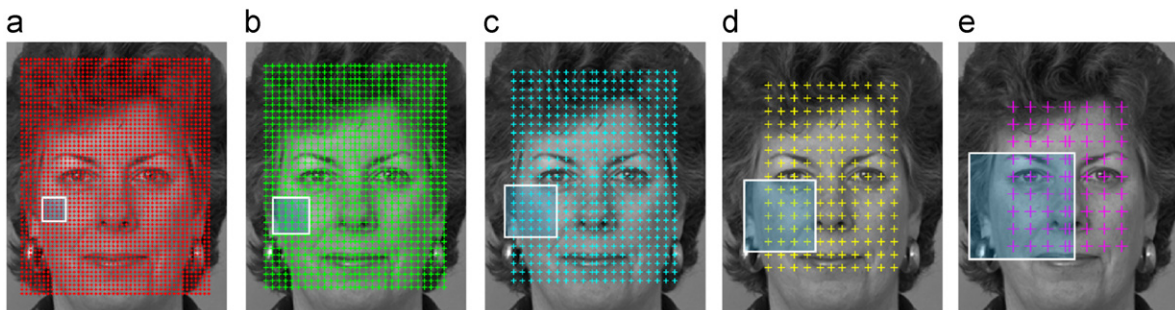**Fig. 2.** . A face from the FERET database with the five grids for spatial scales (a) $v=0$, (b) $v=1$, (c) $v=2$, (d) $v=3$ and (e) $v=4$. The sign + represent the spatial point on the grid where the Gabor wavelet is computed. The white squares represent the size of the Gabor jets for each spatial scale in pixels of (a) 25×25, (b) 37×37, (c) 51×51, (d) 71×71 and (e) 101×101.
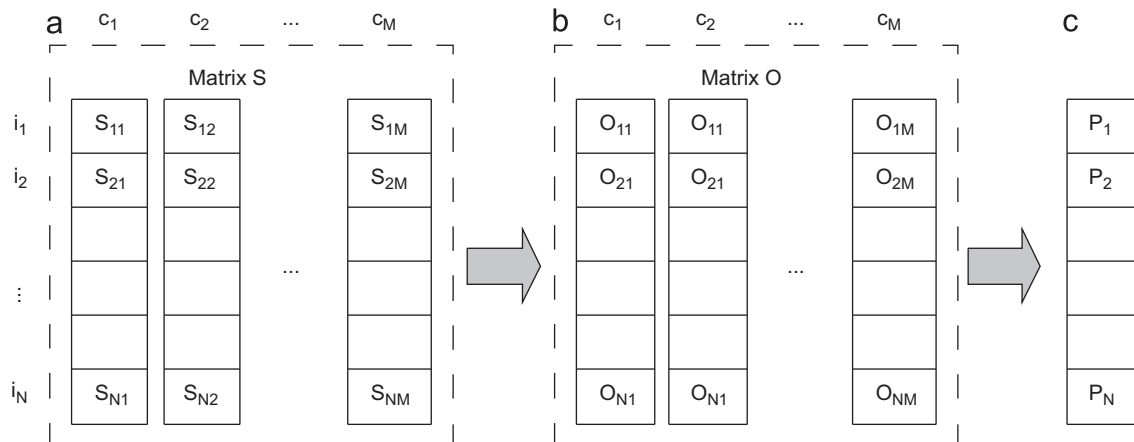
Fig. 3. Illustration of Borda count computation method. (a) Matrix S with dimensions $N \times M$, where S_{ij} is the score of the jth Gabor jet comparison with the ith image of the gallery. (b) Matrix with sorted columns O with dimension $N \times M$ with values $N-1$ to 0 in each column. (c) Borda count score for the ith gallery element as the sum of all column in the ith rows of O.

Table 1
Borda count computation example for a case of a gallery with 4 face images and 6 Gabor jets.

	Matrix S						Matrix O						Matrix P
	c_1	c_2	c_3	c_4	c_5	c_6	c_1	c_2	c_3	c_4	c_5	c_6	
i_1	0.7	0.2	0.6	0.4	0.2	0.7	1	1	2	2	1	2	9
i_2	0.8	0.0	0.1	0.2	0.7	0.1	2	0	0	0	2	0	4
i_3	0.9	0.6	0.9	0.5	0.8	0.6	3	2	3	3	3	1	15
i_4	0.3	0.9	0.2	0.3	0.1	0.8	0	3	1	1	0	3	8

2.2. Databases

2.2.1. The FERET database

The FERET database is the most widely used benchmark for face recognition algorithms [43]. In order to compare our results to other methods, we followed the FERET face recognition protocol that is described in detail in [27]. In the following, we briefly describe the FERET database and the FERET tests. The FERET database has a large number of images with different gesticulations, illumination and a significant amount of time between pictures taken. The FERET database is organized in 5 sets of images: the gallery is Fa, and the test sets are Fb, Fc, Dup1 and Dup2. In the Fa set there are 1196 face images of different people. In the Fb set there are 1195 images of people with different gesticulations. Fc has 194 images with different illumination. In Dup1 there are 722 images of pictures taken between 0 and 34 months of difference with those taken for Fa. The Dup2 set has 234 images taken at least 18 months after the Fa set. Fa set contains one image per person and is the Gallery set, while Fb, Fc, Dup1 and Dup2 are called test sets.

2.2.2. The AR database

The AR database [51] contains frontal faces from 60 females and 76 males. Pictures were taken in two different sessions, with 13 pictures per person per session. Six of the thirteen images contain illumination changes or gesticulation and one image is neutral. In three images the person is wearing sunglasses and in another three images, the person is wearing a scarf.

2.2.3. The Extended Yale B database

The Extended Yale B face database [52,53] contains images from 37 different subjects with varying illumination. Each subject has 65 images illuminated from different angles.

2.2.4. The ORL database

We used the ORL (Olivetti Research Laboratory) faces database [54] for verification. This database contains 400 images of 40 individuals (10 images per individual) with different expressions, limited side movement and limited tilt. The images were captured at different times and with different lighting conditions. The images were manually cropped and rescaled to a resolution of 92×112, 8-bit gray levels.

2.3. Local Gabor enhancements

In the original paper on LMG [43] it was suggested that further improvements could be obtained by jet selection. In fact, it was shown in [43] that a random selection of nearly 50% of the Gabor jets yielded similar results to using all of them. In this paper, we propose two alternative ways of selecting Gabor jets using GAs and entropy information [55]. We also propose enhancements in the Borda count method by weighting the contribution of each voter by the score of the Borda count and by using thresholds to eliminate noisy jet voters. A combination of jet selection and enhanced Borda count is also proposed.

To train, test and compare different methods we use a database for frontal faces with illumination changes, gesticulations and different time difference between the pictures taken for the gallery and the test set. Two sets were used from FERET database: the FERET training set which we call Train1 used in [43,56] that it is a standard partition of FERET with 724 training images. From the total 3880 images in FERET database, we selected 556 images that do not belong to the subsets Fa, Fb, Fc, Dup1 and Dup2 and call it Train2.

2.3.1. Genetic selection of jets (GSJ)

We propose to select jets using a GA where each individual in the population corresponds to a set of selected jets that are coded onto a string with binary elements or chromosome. The jet selection is performed according to the values of the binary elements on the chromosome: if the bit is 1, the jet is selected; if the bit is 0, the jet is not selected. Since in [43] the total number of possible jets applied in the five grids is 4172, the chromosome has a length of 4172 bits. A multi-objective GA was used to maximize the face recognition rate and minimize the number of jets. The GA uses a two-point crossover with a rate of 0.8, uniform mutation with 0.05 probability and 100 individuals per population. An example of jet selection resulting from using GSJ is shown in Fig. 4. Two training sets were used for the GA, Fa–Train1 and Fa–Train2.
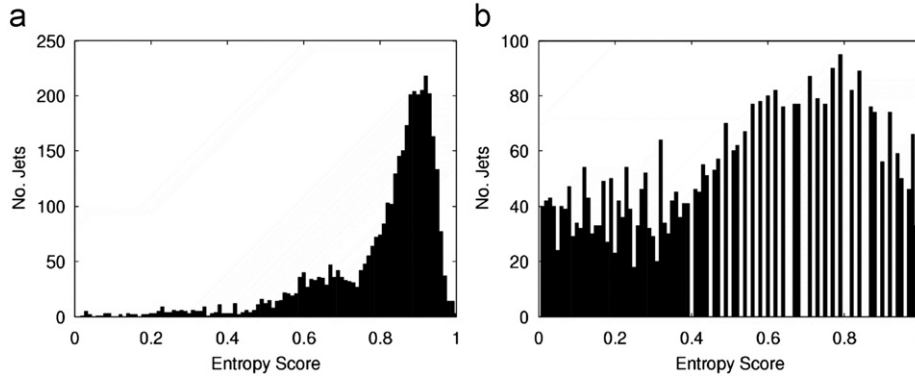
Fig. 4. (a) Entropy histogram for all jets and all of the five wavelengths. (b) Equalized entropy for all jets and all of the five wavelengths.

Table 2
Example with the BIP score computations for the same case presented for the original Borda count of Table 1.

	Matrix S						Matrix O						Matrix $S_{ij}O_{ij}$						Matrix P
	c_1	c_2	c_3	c_4	c_5	c_6	c_1	c_2	c_3	c_4	c_5	c_6	c_1	c_2	c_3	c_4	c_5	c_6	
i_1	0.7	0.2	0.6	0.4	0.2	0.7	1	1	2	2	1	2	0.7	0.2	1.2	0.8	0.2	1.4	4.5
i_2	0.8	0.0	0.1	0.2	0.7	0.1	2	0	0	0	2	0	1.6	0	0	0	1.4	0	3
i_3	0.9	0.6	0.9	0.5	0.8	0.6	3	2	3	3	3	1	2.7	1.2	2.7	1.5	2.4	0.6	11.1
i_4	0.3	0.9	0.2	0.3	0.1	0.8	0	3	1	1	0	3	0	2.7	0.2	0.3	0	2.4	5.6

2.3.2. Entropy based jet selection (EJS)

Entropy [55] is proposed as a tool to select jets that provide maximum information about the face. The goal is to find those jets with the highest entropy because they provide information about what differs from one face to another. Conversely, those jets with low entropy among different face images do not provide information to differentiate faces, and they therefore act as noisy inputs to the classification module. Before the entropy computation, the scores for each jet comparison are normalized to keep the sum of scores P_{ijk} equal to 1, using (2) and (3)

$$P_{ijk} = \frac{S_{ijk}}{\sum_{i'=1}^{N} S_{i'jk}}, \tag{2}$$

$$E_{jk} = -\sum_{i=1}^{N} P_{ijk} \log P_{ijk}, \tag{3}$$

$$\overline{E}_j = \frac{1}{L} \sum_{k=1}^{L} E_{jk}. \tag{4}$$

Indexes i, j and k represent the jth Gabor jet comparison, from the ith gallery image and the kth input image from the test set. S_{ijk} is the score of the jth Gabor jet comparison with the ith image of the gallery and E_{jk} is the entropy of the jth jet of a given kth input image from the test set. The total entropy $\overline{E}_j$ is the average of the entropies of all images computed on the test set (4), where the number of images in the test set is L. $\overline{E}_j$ is a real number and therefore to select those jets with the highest entropy, a threshold T_{hv} is used; then, if $\overline{E}_j > T_{hv}$, the jet is selected. The optimum threshold T_{hv} was chosen for each of the five spatial frequencies using a GA with the same training sets as those in the previous case.

Because the entropy score is not uniformly distributed, the histogram was equalized. For calculation of entropy Train1 was divided in two subsets, the first one with 364 images used as a gallery which we named Train1g and 360 images for test called Train1t. Another entropy score was computed with the gallery Fa and the test Train2.

We constructed histograms to show the jets entropy distribution. Fig. 4(a) shows the jets entropy and Fig. 4(b) shows the equalized jets entropy for all of the five wavelengths together.

The GA used in EJS is similar to the one used in GSJ, with the same training sets (Fa–Train1 and Fa–Train2). A multi-objective GA was used with the same objectives and fitness function, two-point crossover with probability 0.8, uniform mutation of rate of 0.05, and 60 individuals per population. The difference is the length of the chromosome, where each individual has 30 bits (6 bits for each spatial frequency), with thresholds between 0.1 and 0.73.

2.3.3. Borda count enhancement by inclusion of jets inner product value (BIP)

In the standard Borda count method, only jet order determines the final score. In the present paper we propose incorporating the value of the jet inner product (matrix S) in the computation of the final score (matrix P). The final score P for the ith gallery element is $P_i = \Sigma_{j=1}^{M} S_{ij} O_{ij}$. Table 2 shows an example of BIP computation that can be compared to the standard Borda count shown in Table 1.

2.3.4. Borda count enhancement by threshold (BTH)

In the standard Borda count, all jets contribute to the final score even if the inner product value is very small. By using a threshold, T_h, over the scalar product, it is possible to eliminate very small value scores, which act as noise, for the Borda count computation. The jet scores under the threshold are set to zero. If $S_{ij} < T_h$, then $Q_{ij} = 0$, otherwise $Q_{ij} = O_{ij}$, and $P_i = \Sigma_{j=1}^{M} Q_{ij}$. Table 3 shows an example of the Borda count computation with $T_h = 0.55$ that can be compared to the standard Borda count shown in Table 1. The FERET training database was used to obtain the optimum T_h. Using the FERET training set, the rank-1 identification rate was computed varying the T_h threshold between 0.6 and 0.95 as shown in Fig. 8. The area for T_h between 0.80 and 0.89 has significantly better scores than the rest; therefore, the T_h selected from this region was 0.81 which was the maximum for the training database.

Table 3
Example of the BTH score computation for the original Borda count of Table 1.

	Matrix S						Matrix O						Matrix Q						Matrix P
	c_1	c_2	c_3	c_4	c_5	c_6	c_1	c_2	c_3	c_4	c_5	c_6	c_1	c_2	c_3	c_4	c_5	c_6	
i_1	0.7	0.2	0.6	0.4	0.2	0.7	1	1	2	2	1	2	1	0	2	0	0	2	5
i_2	0.8	0.0	0.1	0.2	0.7	0.1	2	0	0	0	2	0	2	0	0	0	2	0	4
i_3	0.9	0.6	0.9	0.5	0.8	0.6	3	2	3	3	3	1	3	2	3	0	3	1	12
i_4	0.3	0.9	0.2	0.3	0.1	0.8	0	3	1	1	0	3	0	3	0	0	0	3	6

2.4. Combination of Gabor jets selection and enhanced Borda count

The proposed individual enhancements, EJS, GJS, BIP and BTH, were combined and optimized in cascade using a GA to improve face recognition results. We tested several combinations of individual enhancements as follows: EJS–BTH, EJS–BIP and EJS–BTH–BIP.

2.5. Face recognition under illumination changes, occlusion and pose variation

We tested the LMG method under illumination changes, occlusion and pose variation using available face databases and compare the results with those published in international studies [38,32]. For this purpose we used the Extended Yale B and AR databases for illumination changes, the AR database for occlusion and the FERET database (subsets: bd, be, bf and bg) for pose variation.

2.5.1. Face recognition with illumination changes
We tested the LMG method under significant illumination changes using face database AR and Extended Yale B. In order to compare our results to those previously published, we followed the methods according to [32].

For the Extended Yale B database, we employed a gallery of 32 images per person and a testing set of 33 images per person for a total of 37 people. A second partition was performed on Extended Yale B with only 2 images per person in the gallery. The test set was composed of 63 images per subject. For the AR face database, 50 men and 50 women from the database were selected and the gallery contained 7 images per person. The test set contained a different set of 7 images per person.

2.5.2. Face recognition with occlusions
As in [32] we tested the LMG method with faces occluded by sunglasses and scarves on the AR face database. As in Section 2.5.1, we used images from 50 men and 50 women from the AR database.

(i) Scarf occlusion: The testing set contains 6 images per person, i.e., a total of 600 images, with faces occluded by scarves. The gallery is the same as in Section 2.5.1, and the GA training is performed with images from session 1.
(ii) Sunglasses occlusion: Testing was performed using 3 images with sunglasses per person from session 2, i.e., a total of 300 images. The gallery is the same as in Section 2.5.1.

2.5.3. Face recognition with pose variation
We tested the LMG method on face recognition with pose variation as in [33,57,58]. We used the subsets bd, be, bf and bg of the FERET database [27] and use the frontal image from Fa in the gallery. Therefore, images with frontal faces in the gallery are compared to pose variations in bd, be, bf and bg. The subsets bd, be, bf and bg include pose variations for angles $25°$, $15°$, $-15°$ and $-25°$, respectively. Although these are small pose variations cover

several possible applications for face recognition in access control and watch list.

2.6. Face verification

Face verification is a very important tool for person authentication and it is of significant value in security. Following the same method as in [18] and using the ORL (Olivetti Research Laboratory) face database [54], face verification was performed with our LMG method and compared to results published with other methods. The ORL database contains 400 images of 40 individuals (10 images per individual). As in [18], we used 5 images per individual for gallery (faces 1–5) and 5 faces for testing (faces 6–10), with a total of 200 images for gallery and 200 for testing. We also used the Detection Cost Function (DCF) [59] to compare with other methods

$$DCF = C_{miss} \times P_{miss} \times P_{true} + C_{fa} \times P_{fa} \times P_{false} \quad (5)$$

where C_{miss} is the cost of a wrong rejection, C_{fa} is the cost of a wrong acceptance, P_{true} is the a priori probability of each individual (1/40 in the ORL case) and $P_{false} = 1 - P_{true}$. We use $C_{miss} = C_{fa} = 1$. For verification with the LMG, it is necessary to compare the inner product result between one individual of the testing set and only one individual of the gallery. To determine whether an individual of the testing set matches the selected one in the gallery, we compute

$$V_i = \frac{1}{M} \sum_{j=1}^{M} S_{ij}. \quad (6)$$

If an image i exists such as $V_i > T$, where T is a threshold between 0 and 1, then the individual of the testing set is verified as the one selected.

3. Results

With the objective of comparing our results to previous work, we summarized the results of our literature review on local matching Gabor methods in the following section. One of the papers in print [48] provides an up to date summary highlighting the best results reached in face recognition with local Gabor methodology.

3.1. Previously published results on local Gabor

Our literature review on face recognition is summarized in Table 4. This table shows the best results on face recognition published in nine recent papers. The first four columns of the table show the face recognition rate for different subsets of the FERET database. The next four columns show the approximate number of errors on the same subsets of the FERET database. The last column shows the total number of errors on all subsets of the FERET database. It can be observed that the best result with the smallest number of total errors in all subsets is the LMG method [43].

Table 4
Rank-1 face recognition rate on different subsets of FERET database for different face recognition algorithms published in the literature.

Methods	Accuracy (%)				Number of errors				
	Fb	Fc	Dup1	Dup2	Fb	Fc	Dup1	Dup2	Total
LMG [43][a]	**99.5**	**99.5**	**85.0**	79.5	**6**	**1**	**108**	48	**163**
LGBPWP [41][a]	98.1	98.9	83.8	**81.6**	23	2	117	**43**	185
Weighted LLGP_FR [40][a]	99.0	99.0	80.0	78.0	12	2	144	51	209
Weighted HGPP [38][a]	97.5	99.5	79.5	77.8	30	1	148	52	231
Weighted LGBPHS [37][a]	98.0	97.0	74.0	71.0	24	6	188	68	286
LGT [39][a]	97.0	90.0	71.0	67.0	36	19	209	77	341
Weighted LBP [37,26][a]	97.0	79.0	66.0	64.0	36	41	245	84	406
GFC [37,35][b]	97.2	79.9	68.3	46.6	33	39	229	125	426
EBGM [37,34][b]	95.0	82.0	59.1	52.1	60	35	295	112	502

[a] Results extracted from original source
[b] Results extracted from the first referenced paper, and the original method is the second referenced paper.

Table 5
Face recognition rate on different subsets of the FERET database for our proposed methods and compared to the best results published up to date in the literature LMG [43]. Subindex 1 indicates FERET training set Train1, subindex 2 indicates FERET training set Train2.

Methods	Accuracy (%)				Number of errors				
	Fb	Fc	Dup1	Dup2	Fb	Fc	Dup1	Dup2	Total
LMG [43]	99.5	99.5	85.0	79.5	6	1	108	48	163
LMG–GSJ$_1$	99.7	99.5	86.3	81.2	4	1	99	44	148
LMG–GSJ$_2$	99.7	99.5	86.3	82.1	3	1	99	42	145
LMG–EJS$_{1a}$	**99.8**	**100**	**88.0**	84.2	**2**	**0**	**87**	37	126
LMG–EJS$_{1b}$	99.4	99.5	**88.0**	87.2	7	1	**87**	30	125
LMG–EJS$_2$	99.5	99.5	87.0	85.9	6	1	94	33	134
LMG–BIP$_1$	99.6	99.5	86.0	82.9	5	1	101	40	147
LMG–BTH$_1$	99.7	99.5	86.8	82.1	4	1	95	42	142

3.2. Results of proposed enhancements

Table 5 summarizes the most important results obtained with the different methodological enhancements proposed in this paper. The best result published in the literature [43] is shown on the first line. The first four columns of Table 5 show the results in % and the next four columns show the number of errors for each subset of the FERET database. The last column shows the total number of errors in all subsets of the FERET database. In the case of LMG [43], the total number of errors in all subsets is 163.

3.2.1. Results for GSJ

Table 5 shows the best result published for LMG [43] on the first row. Table 5 also shows the best results obtained for the jet selection using GSJ, LMG–GSJ$_1$ was trained with Train1 and GSJ$_2$ with Train2. Results show a small improvement in Fb subset (recognized 2 additional faces). Results were the same for the Fc subset compared to the original results in LMG [43]. Nevertheless, on subsets Dup1 and Dup2, results improved 1.3% (9 fewer errors) and 2.1% (6 fewer errors, for LMG–GSJ$_2$). In summary, for GSJ it is possible to recognize 18 additional faces compared to LMG [43] using half the number of jets. The reduction in the number of jets is significant because it allows faster processing for real-time computation. Fig. 5 shows a selection of jets resulting from the GA.

3.2.2. Results for EJS

Table 5 shows on lines LMG–EJS$_{1a}$, LMG–EJS$_{1b}$ trained with Train1 and LMG–EJS$_2$ trained with Train2, the best results obtained for the jet selection using entropy information. The best result for LMG–EJS$_{1b}$ shows an improvement of 0.1% (1 case) for Fb subset, no improvement for Fc subset, 3% (21 fewer errors) for Dup1 and 7.7%

(18 fewer errors) for Dup2, compared with LMG [43]. EJS$_2$ was trained with Train2 and showed significant improvements in recognition rate in the subsets Dup1 and Dup2, reaching an increment between 2% and 6.4%. The total number of errors was reduced from 163 to 125 using EJS. This represents a total improvement of 38 faces compared to LMG. Fig. 6 shows the equalized entropy for each spatial frequency. Fig. 7 shows an example of the jets selected by entropy with solution LMG–EJS$_2$.

The total number of jets in the LMG method is 4172, but there is a different number of jets due to the filter size at each spatial frequency, i.e., 2420 jets for $v=0$, 1015 jets for $v=1$, 500 jets for $v=2$, 165 jets for $v=3$ and 72 jets for $v=4$. The percentage of selected jets using EJS$_{1a}$ was 86% for $v=0$, 33% for $v=1$, 32% for $v=2$, 96% for $v=3$ and 81% for $v=4$. In the case of EJS$_2$ the percentage of selected jets for each spatial frequency was 24% for $v=0$, 76% for $v=1$, 32% for $v=2$, 56% for $v=3$ and 82% for $v=4$. Also, it can be observed that LMG–EJS$_2$ improved more in subsets Dup1 and Dup2 rather than in subsets Fb and Fc. On the contrary, the other solution, LMG–EJS$_1$, improved more in the Fb and Fc subsets than in Dup1 and Dup2, although the total improvement was less than LMG–EJS$_2$.

3.2.3. Results for BIP

Table 5, line LMG–BIP$_1$ shows the results obtained by including the inner product score value into the Borda count computation. The recognition rate improvement compared with the original LMG method, was 0.1% for Fb (1 less error), same result for Fc, 1% (7 fewer errors) for Dup1 and 3.4% (8 fewer errors) in Dup2. The total number of errors was reduced from 163 to 147 using BIP. The total improvement was of 16 faces compared to LMG.

3.2.4. Results for Borda count enhancement by threshold (BTH)

The rank-1 face recognition rate is shown in Table 5 as LMG–BTH$_1$. The average result obtained for T_h in the interval 0.80–0.89 was Fb 99.7, Fc 99.5, Dup1 86.8 and Dup2 82.1%, with only 142 errors in total versus 163 cases in the original LMG method. Fig. 9 shows the face recognition accuracy for FERET database using different thresholds in the interval 0.80–0.89. Using BTH, the total number of errors was reduced from 163 to 142.

3.3. Combined methods

A selection of the best results obtained for combined enhancements is presented in Table 6. The results of the best paper published in the literature for the LMG method are on the first line of Table 6. It can be observed that there are several combinations of the proposed methods that yield better results than those
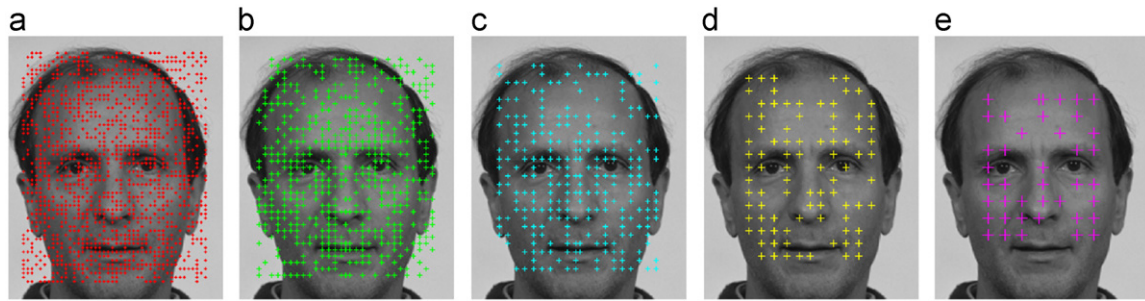
Fig. 5. Selection of jets for each spatial frequency, (a) $v=0$, (b) $v=1$, (c) $v=2$, (d) $v=3$ and (e) $v=4$, using GA. The total of jets selected is 2094, 50.19% of them, which means a 55% of computation time.
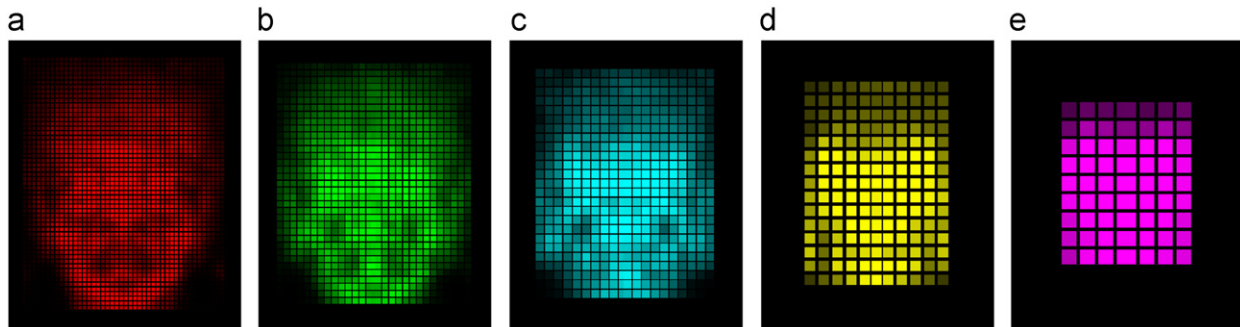

Fig. 6. Computed equalized entropy for jets at five spatial frequencies (a) $v=0$, (b) $v=1$, (c) $v=2$, (d) $v=3$ and (e) $v=4$. The color represents different spatial frequencies, and the increased brightness represents higher entropy. (For interpretation of the references to color in this figure legend, the reader is referred to the web version of this article.)
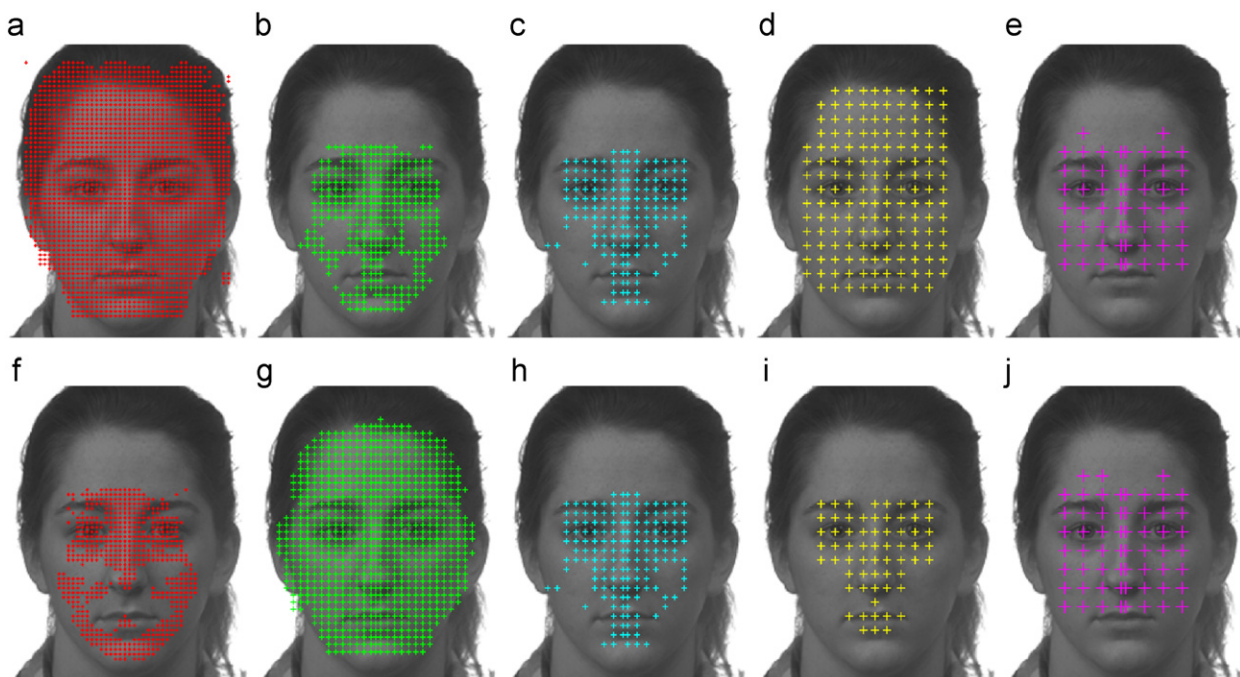

Fig. 7. Selection of jets for the five spatial frequencies, (a)–(f) $v=0$, (b)–(g) $v=1$, (c)–(h) $v=2$, (d)–(i) $v=3$ and (e)–(j) $v=4$, using entropy (EJS). (a)–(e) are selection EJS$_1$ and (f)–(j) EJS$_2$.

obtained for each improvement alone. For example the best case trained with Train1 consists of LMG–EJS–BTH–BIP$_{1b}$ with a total number of 112 errors compared to 163 using LMG, while the best case with Train2 LMG–EJS–BTH–BIP$_2$ had 122 errors. This represents a 31% and a 25% improvement relative to the LMG method. Other combinations such as LMG–GSJ–BTH–BIP$_1$, LMG–EJS–BTH$_1$ and LMG–EJS–BIP$_1$ yield a total number of errors of 140, 116 and 126, respectively, which represent a 14%, 29% and 23% improvement relative to the LMG method. This proves that there are several alternatives with fewer numbers of jets that achieve significant improvements in classification rate with a decrease in computational time.

3.4. Results in face recognition under illumination changes, occlusion and pose variation

3.4.1. Face recognition with illumination changes results

We use Extended Yale B to test the LMG method with images under significant illumination changes. Four different random

Fig. 8. Face recognition rate in training set as a function of the threshold T_h for BTH.

partitions of the gallery and test were performed (p1, p2, p3 and p4), as shown in Table 7. Results are in the range between 99.1% and 99.8%. In Table 7 p0 corresponds to the partition used in [32]. As shown in Table 7, similar results were obtained with LMG–EJS–BIP–BTH. With the partition formed by 2 images in the gallery and 63 images per subject in the test, results were 99.9% for LMG and 99.8% for LMG–EJS–BIP–BTH.

Table 8 shows the test results over the AR database for the LMG method and methods in [32]. It can be observed that highest scores are reached by the LMG–EJS–BIP–BTH method.

In the original LMG paper [43], the authors explain that Gabor filters are robust to illumination changes because the filters can detect spatial frequencies independently from amplitude, i.e., Gabor filters tend to extract higher frequency components. This argument is strengthened by the finding that most illumination changes in images are contained in the low spatial frequency domain [60]. In the case of the discrete cosine transform (DCT) method for illumination compensation, low frequencies are filtered out to improve face recognition under illumination changes [60,61]. Furthermore, each Gabor feature in the test image is compared locally with the corresponding Gabor feature in the gallery which provides additional robustness to illumination changes, gesticulations and partial occlusions [40]. The high accuracy obtained in face recognition results with our proposed method is not an isolated finding. Several previous publications have reached good results employing Gabor filters with illumination changes and gesticulations [38–41,62], and therefore our
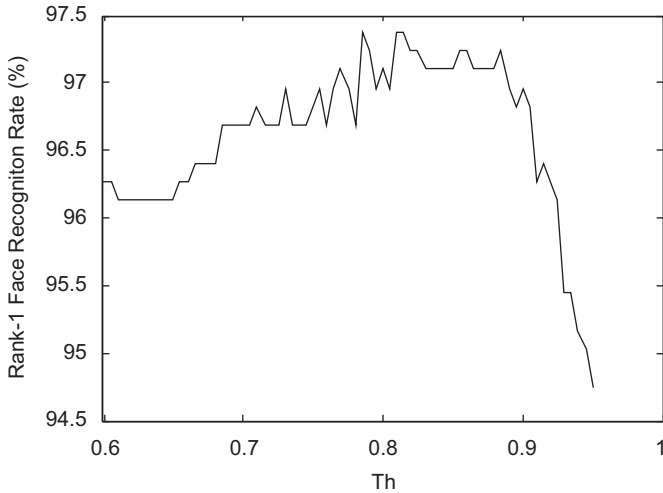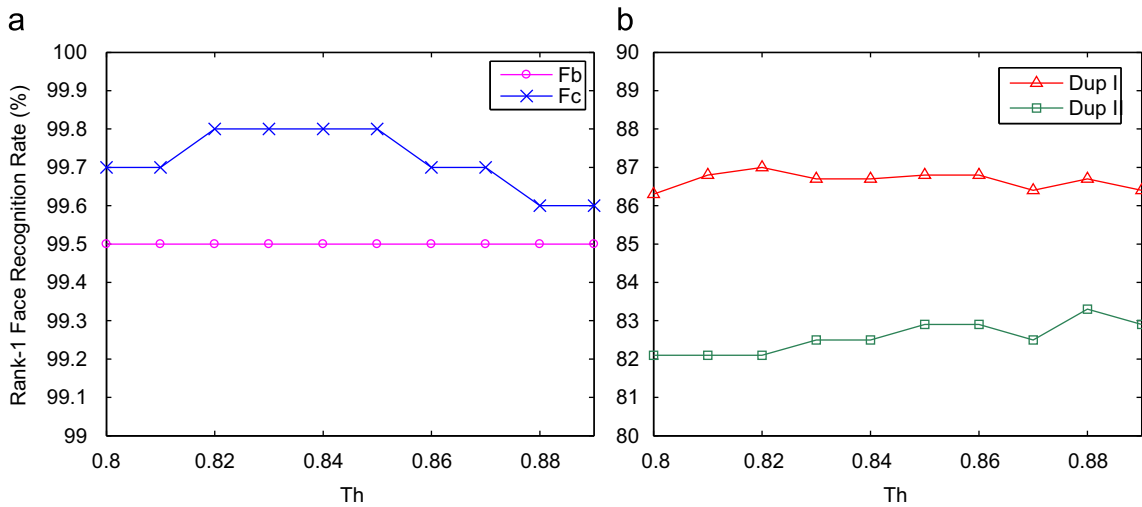

Fig. 9. Face recognition rate in FERET for T_h between 0.8 and 0.89.

Table 6
Face recognition rate on different subsets of the FERET database for our proposed methods combined and compared to the best results published up to date in the literature LMG [43]. Subindex 1 indicates FERET training set Train1, subindex 2 indicates FERET training set Train2.

Methods	Accuracy (%)				Number of errors				
	Fb	Fc	Dup1	Dup2	Fb	Fc	Dup1	Dup2	Total
LMG [43][a]	99.5	99.5	85.0	79.5	6	1	108	48	163
LMG–GSJ–BTH–BIP$_1$	99.7	99.5	86.6	83.8	4	1	97	38	140
LMG–GSJ–BTH–BIP$_2$	99.6	99.5	86.8	83.8	5	1	95	38	139
LMG–EJS–BTH$_1$	**99.8**	99.5	88.9	85.9	**2**	1	80	33	116
LMG–EJS–BTH$_2$	99.5	**100**	88.1	86.3	6	**0**	86	32	124
LMG–EJS–BIP$_1$	99.5	**100**	87.8	86.3	6	**0**	88	32	126
LMG–EJS–BIP$_2$	99.2	99.5	87.4	86.3	10	1	91	32	134
LMG–EJS–BTH–BIP$_{1a}$	99.5	**100**	88.8	**87.6**	6	**0**	81	**29**	116
LMG–EJS–BTH–BIP$_{1b}$	**99.8**	99.5	**89.2**	86.8	2	1	**78**	31	112
LMG–EJS–BTH–BIP$_2$	99.6	**100**	88.2	86.3	5	**0**	85	32	122

[a] Results extracted from original source.

Table 7
Results of face recognition with illumination changes on the Extended Yale B database.

	Accuracy (%)				
	p0	p1	p2	p3	p4
SRC [32]	98.1	–	–	–	–
LMG	–	99.3	99.8	99.6	99.1
LMG–EJS–BIP–BTH	–	99.4	99.4	99.5	99.5

Table 8
Results of face recognition with illumination changes and occlusion with sunglasses and scarves on the AR database.

	Accuracy (%)		
	Normal	Sunglasses	Scarves
LGBPHS [37]	–	80	98
SRC [32]	95.7	97.5	93.5
LMG	98.6	97.7	97.2
LMG–EJS–BIP–BTH	99.1	98.0	99.0

Table 9
Results of face recognition on the subsets with pose variation bd, be, bf and bg of the FERET database.

	Accuracy (%)			
	bd	be	bf	bg
LMG	81.0	97.0	98.0	79.5
LMG–EJS–BIP–BTH	93.5	98.5	98.0	91.5

results are an improvement in accordance with those previously reported results.

3.4.2. Face recognition with occlusions results

Table 8 shows the test results on the AR face database for occlusions with sunglasses and scarves. In both types of occlusions, the LMG–EJS–BIP–BTH method reached slightly higher results than other previously published for the AR database.

3.4.3. Recognition with pose variation results

We tested the LMG and LMG–EJS–BIP–BTH methods with the subsets bd, be, bf and bg of the FERET database. Table 9 shows the results of face recognition for small pose variations. Results range from 91.5% to 98.5% for the different FERET subsets.

In the Methods Section 2.1, we explained that in the LMG method [43], the first step toward face recognition is face localization, normalization and alignment. As in [43], we use the eyes for face alignment both in the gallery and in the test set. The normalized image has the eyes fixed at positions (67, 125) and (135, 125) within a 203×251 pixels image [43]. We use the ground truth marks in the eyes for alignment. In the past few years, several methods for accurate eye localization have been developed with accuracy over 99% for faces with small pose variations [8,11]. Therefore, face alignment is not a major issue for small pose variations. In cases of larger pose variation, other fiducial points, e.g., nose, mouth corners, eye corners, etc., may be used for alignment.

Our results have been compared with other six papers based on Gabor features that reach results over 95% on Fb and over 90% on Fc of the FERET database [37–41,43], which shows that our results

correspond to an improvement respect to previous publications. As LMG [43], most face recognition methods show good performance to small pose variations ($\sim 15°$) [5,63]. Recognition rate falls to 80% for the LMG method applied to faces with poses around 25°. Nevertheless, by incorporating our paper proposed EJS jet selection, recognition rate are around 91–93%. The EJS selection is shown in Fig. 7 and by comparison to the original LMG jet location shown in Fig. 2, it can be observed that the EJS selection is confined to the central part of the face where matching among jets is better for slight pose rotations. As explained in Section 2, face images are aligned with the eye position and normalized in size. Therefore, jets from similar regions are compared for the test and gallery images. Fig. 10(a) shows on the first column, the frontal gallery image and from the second up to the fifth column, face poses for $-25°$, $-15°$, 15° and 25°, for the same subject. Fig. 10(a) shows for the frontal gallery image two rows with test images for spatial frequencies λ_2 and λ_4 (2 of the 5λs). Over the test images the EJS jet positions are shown as a bright dot. Fig. 10(a) also shows the jets scores above a threshold of 0.85 as a bright square over each jet position for the test images and the gallery image. In case that most jets yield high scores, the face will be covered with bright squares. It can be observed that most jet scores are very high for face poses at $-15°$ and 15° and that high scores decrease slightly for face poses at $-25°$ and 25°. Fig. 10(a) may help to explain our results of 98% matching for poses between $-15°$ and 15°, and the fall to 91% for poses at $-25°$ and 25°. Fig. 10(b) shows the results of comparing the test images to a different subject in the gallery. It can be observed that a significant number of jet scores are below the threshold 0.85 and therefore, the voting process will yield the correct face recognition for this subject. It has to be emphasized that we use this arbitrary score of 0.85 only to illustrate the jets matching process.

3.5. Face verification results

Table 10 shows the DCF value for different face recognition methods: Eigenfaces [14], KLT [64], DCT [16] and WHT [18], including the result for our method. Our results, LMG-verif, are better than those published in [18]. In Table 10 our result is compared to eigenfaces, KLT, DCT and WHT for the same database [18].

3.6. Computational time for jet selection

Jet selection has two important results, the first one, is to improve recognition rate and the second, to reduce computational time. Improving jet selection produces two important results: an increased recognition rate and reduced computational time. If fewer jets are computed, the computational time decreases. Table 11 shows, on the first column, the total number of jets used (4172) and the number of jets of four different jet selections. On the second column is the ration between the number of jets using the jet selection and the total number of jets. The third column shows the ratio between the computational time employed in each selection over the time employed with all the jets. It can be observed that a 45% reduction of computational time was obtained for the first two selections. The computational time required for the total number of 4172 jets is 48 ms on a PC with an Intel Quad Core-2.66 GHz CPU, 2 GB RAM using C++ under Windows XP SP2 with multithreading. For a jet selection of 1909 jets the computational time is 27 ms and for a jet selection of 2577 jets 30 ms. The measured computational time allows real-time processing which is necessary for many applications.
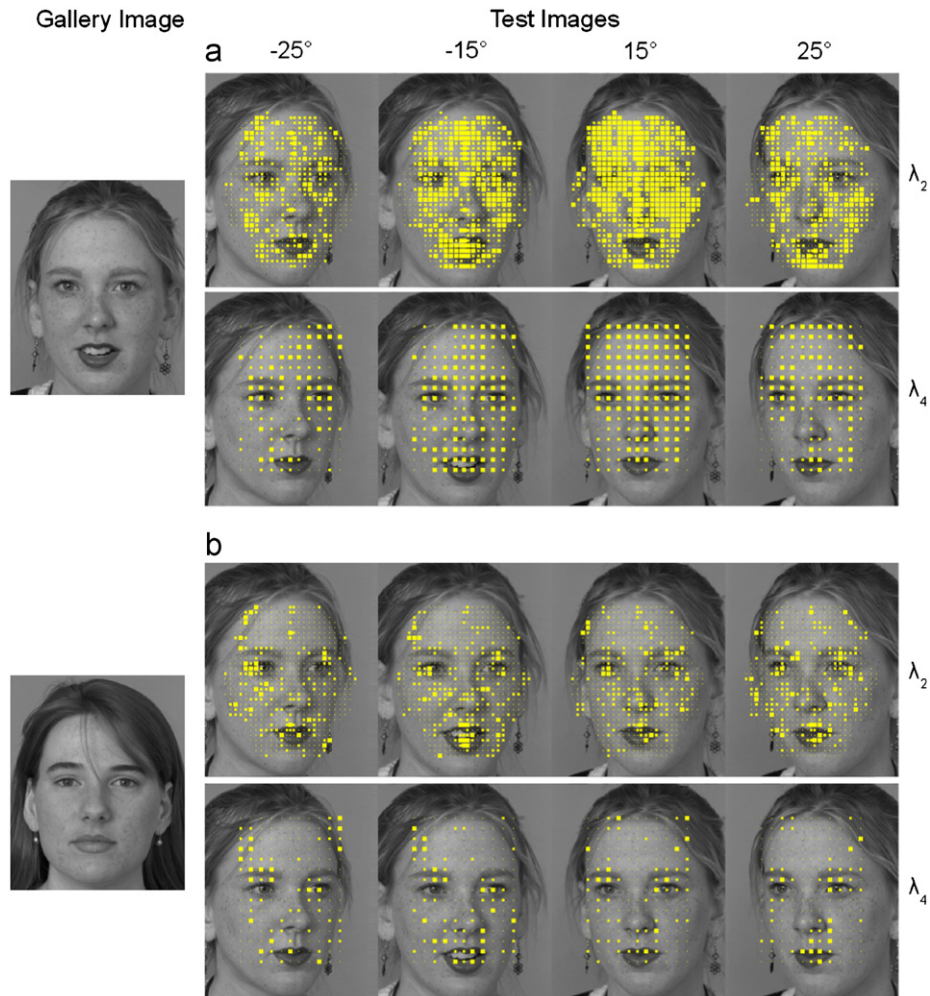
Fig. 10. Illustration of jet scores for the test images and gallery image from (a) the same person and (b) closest subject in the gallery. Jet positions from the EJS are shown as a bright point on the test images for two spatial frequencies λ_2 and λ_4. Jet scores above a threshold of 0.85 are shown as a bright square over each jet position. (a) Most jet scores are very high for face poses at $-15°$ and $15°$ and high scores decrease slightly for face poses at $-25°$ and $25°$. (b) Results of comparing the test images to a different subject in the gallery. A significant number of jet scores are below the threshold 0.85 and therefore, the voting process will yield the correct face recognition with higher scores of (a).

Table 10
Minimum verification error result for the ORL face database using the DCF cost function for different methods including our LMG-verif.

Transform	Min(DCF) (%)
Eigenfaces[a]	6.99
KLT[a]	5.24
DCT[a]	5.23
WHT[a]	6.05
LMG-verif	4.93

[a] Results extracted from [18].

Table 11
Shows, on the first column, the total number of jets and the number of jets for four different jet selections. The second column shows the ratio between the total number of jets and each of the four jet selections. The third column shows the ratio of the computational time employed between the total number of jets and each of the four jet selections.

Method	Number of jets	Ratio between no. of jets	Ratio between computational time
Base	4172	1	1
Selection_1	2094	0.50	0.55
Selection_2	2111	0.51	0.55
Selection_3	3367	0.81	0.80
Selection_4	2186	0.52	0.58

4. Conclusions

Face recognition is an important topic for surveillance, man-machine interfaces and selective marketing. Several recent studies have shown the predominance of local matching approaches in face recognition results. Real-time implementation of local matching methods is possible but it is important to reduce the number of computations by reducing the number of points used for computation. We propose several methodological enhancements to the local matching Gabor method and show results that improve face recognition rate to achieve the highest scores for facial recognition published to date in the literature.

Results of the methodological improvements proposed in this paper show that it is possible to improve face recognition rate by selecting jets with genetic, GSJ, or entropy, EJS, based methods. Both methods, GSJ and EJS, produce more significant improvements in the subset Dup1 (up to 34 month difference) and Dup2 (at least 18 month difference) where images from the same person were taken further apart in time. The largest improvement by a single proposed method was with entropy jet selection (LMG–EJS$_2$) that reduced the total number of errors in face recognition from 163 to

125, a 23% improvement. The use of fewer jets has also important impact in real-time implementation of these methods.

Both proposed methods BIP and BTH produced more significant improvements in the subsets Dup1 and Dup2 where images from the same person were taken further apart in time. By using the BTH method, the total number of errors decreased from 163 to 142 (a 12.9% error reduction) and for BIP the total number of errors decreased from 163 to 147 (a 9.8% error reduction).

It was shown that it is possible to obtain even better results by combination of the proposed methods in cascade. There are several alternatives available to combine the methods. For example, LMG–EJS–BTH reached only 116 errors (a 28% error reduction), LMG–EJS–BTH–BIP reached 112 errors (a 31% error reduction).

We also tested the proposed method under illumination changes, occlusions with sunglasses and scarves and for small pose variations. Results on two different face databases (AR and Extended Yale B) with significant illumination changes showed over 90% recognition rate. The combination LMG–EJS–BTH–BIP reached 98% and 99% recognition rate in images with sunglasses and scarves from the AR database, respectively. The proposed method reached 93.5% recognition on faces with small pose variation of $25°$ rotation and 98.5% with 15% rotation in the FERET database.

Acknowledgements

Appendix A. Supplementary materials

Supplementary data associated with this article can be found in the online version at doi:10.1016/j.patcog.2010.10.017.

References

[1] http://www.tfl.gov.uk/corporate/media/newscentre/archive/11756.aspx.
[2] http://www.telegraph.co.uk/news/worldnews/europe/france/3209808/Paris-to-quadruple-number-of-CCTV-cameras.html.
[3] http://www.metromadrid.es/es/comunicacion/prensa/noticia205.html.
[4] http://www.metrosantiago.cl/sala_prensa_detalle.php?c=4c5bde74a8f11065 6874902f07378009.
[5] X. Zhang, Y. Gao, Face recognition across pose: a review, Pattern Recognition 42 (2009) 2876–2896.
[6] S. Mason, Is there a need for identity cards? Computer Fraud & Security 9 (2004) 8–14.
[7] H.H. Liu, C.S. Ong, Variable selection in clustering for marketing segmentation using genetic algorithms, Expert Systems with Applications 34 (1) (2008) 502–510.
[8] P. Campadelli, R. Lanzarotti, G. Lipori, Precise eye and mouth localization, International Journal of Pattern Recognition and Artificial Intelligence (IJPRAI) 23 (3) (2009) 359–377.
[9] C. Perez, V. Lazcano, P. Estevez, C. Held, Real-Time Template Based Face, Iris detection on rotated faces, International Journal of Optomechatronics 3 (1) (2009) 54–67.
[10] C.A. Perez, V.A. Lazcano, P.A. Estévez., Real-time Iris detection on coronal-axis-rotated faces, IEEE Transactions on Systems, Man and Cybernetics—Part C: Applications and Reviews 37 (5) (2007) 971–978.
[11] C.A. Perez, C.M. Aravena, J.I. Vallejos, P.A. Estevez, C.M. Held, Face and Iris localization using templates designed by particle swarm optimization, Pattern Recognition Letters 31 (2010) (2010) 857–868.
[12] C.A. Perez, C.A. Salinas, P.A. Estevez, P.M. Valenzuela, Genetic design of biologically inspired receptive fields for neural pattern recognition, IEEE Transactions on Systems Man and Cybernetics Part B—Cybernetics 33 (2) (2003) 258–270.
[13] C.A. Perez, G.D. Gonzalez, L.E. Medina, F.J. Galdames, Linear versus nonlinear neural modeling for 2-D pattern recognition, IEEE Transactions on Systems Man and Cybernetics Part A—Systems and Humans 35 (6) (2005) 955–964.
[14] M. Turk, A. Pentland, Face recognition using eigenfaces, in: Proceedings IEEE Conference on Computer Society, CVPR '91, Maui, HI, USA, 1991, pp. 586–591.
[15] P. Belhumeur, J Hespanha, D. Kriegman, Eigenfaces vs. fisherfaces: recognition using class specific linear projection, IEEE Transactions on Pattern Analysis and Machine Intelligence 19 (7) (1997) 711–720.
[16] C. Podilchuk, X. Zhang, Face recognition using DCT-based feature vectors, in: Proceedings IEEE International Conference on Acoustics, Speech and Signal Processing ICASSP'96, Washington, DC, USA, 1996, vol. 4, pp. 2144–2147.
[17] Z.M. Hafed, M.D. Levine, Face recognition using discrete cosine transform, International Journal of Computer Vision 43 (3) (2001) 167–188.
[18] M. Faundez-Zanuy, J. Roure, V. Espinosa-Duro, J.A. Ortega, An efficient face verification method in a transformed domain, Pattern Recognition Letters 28 (7) (2007) 854–858.
[19] B. Li, C.-H. Zheng, D.-S. Huang, Locally linear discriminant embedding: an efficient method for face recognition, Pattern Recognition 41 (12) (2008) 3813–3821.
[20] S.T. Roweis, L.K. Saul, Nonlinear dimensionality reduction by locally linear embedding, Science 290 (5500) (2000) 2323–2326.
[21] L.K. Saul, S.T. Roweis, Think globally, fit locally: unsupervised learning of low dimensional manifolds, Journal of Machine Learning Research 4 (2003) 119–155.
[22] F. Wang, J. Wang, C. Zhang, J. Kwok, Face recognition using spectral features, Pattern Recognition 40 (10) (2007) 2786–2797.
[23] B. Schölkopf, A. Smola, K. Müler, Nonlinear component analysis as a kernel eigenvalue problem, Neural Computation 10 (1998) 1299–1319.
[24] M. Kyperountas, A. Tefas, I. Pitas, Dynamic training using multistage clustering for face recognition, Pattern Recognition 41 (3) (2008) 894–905.
[25] E.P. Vivek, N. Sudha, Robust Hausdorff distance measure for face recognition, Pattern Recognition 40 (2) (2007) 431–442.
[26] T. Ahonen, A. Hadid, M. Pietikäinen, Face description with local binary patterns: application to face recognition, IEEE Transactions on Pattern Analysis and Machine Intelligence 28 (12) (2006) 2037–2041.
[27] P.J. Phillips, H. Moon, S.A. Rizvi, P.J. Rauss, The FERET database and evaluation procedure for face recognition algorithms, Image and Vision Computing 16 (5) (1998) 295–306.
[28] F. Bianconi, A. Fernández, Evaluation of the effects of Gabor filter parameters on texture classification, Pattern Recognition 40 (2007) 3325–3335.
[29] D. Gabor, Theory of communication, Journal of Institute for Electrical Engineering 93 (III/26) (1946) 429–457.
[30] V. Kyrki, J.-K. Kamarainen, H. Kälviäinen, Simple Gabor feature space for invariant object recognition, Pattern Recognition Letters 25 (2004) 311–318.
[31] M. Lades, J.C. Vorbrüggen, J. Buhmann, J. Lange, C.v.d. Malsburg, R.P. Würtz, W. Konen, Distortion invariant object recognition in the dynamic link architecture, IEEE Transactions on Computers 42 (3) (1993) 300–310.
[32] J. Wright, A.Y. Yang, A. Ganesh, S.S. Sastry, Y. Ma, Robust face recognition via sparse representation, IEEE Transactions on Pattern Analysis and Machine Intelligence 31 (2) (2009) 210–227.
[33] A. Wagner, J. Wright, A. Ganesh, Z. Zhou, Y. Ma, Towards a practical face recognition system: robust registration and illumination by sparse representation, in: IEEE Conference on Computer Vision and Pattern Recognition CVPR 2009, 2009, pp. 597–604.
[34] L. Wiskott, J.-M. Fellous, N. Kruger, C. v. d. Malsburg, Face recognition by elastic bunch graph matching, IEEE Transactions on Pattern Analysis and Machine Intelligence 19 (7) (1997) 775–779.
[35] C. Liu, H. Wechsler, Gabor feature based classification using the enhanced Fisher linear discriminant model for face recognition, IEEE Transactions on Image Processing 11 (4) (2002) 467–476.
[36] C. Liu, H. Wechsler, Robust coding schemes for indexing and retrieval from large face databases, IEEE Transactions on Image Processing 9 (1) (2000) 132–137.
[37] W. Zhang, S. Shan, W. Gao, X. Chen, H. Zhang, Local Gabor binary pattern histogram sequence (LGBPHS): a novel non-statistical model for face representation and recognition, in: Proceedings of the Tenth IEEE International Conference on Computer Vision, Beijing, China, 2005, pp. 786–791.
[38] B. Zhang, S. Shan, X. Chen, W. Gao, Histogram of Gabor phase patterns (HGPP): a novel object representation approach for face recognition, IEEE Transactions on Image Processing 16 (1) (2007) 57–68.
[39] Z. Lei, S. Li, R. Chu, X. Zhu, Face recognition with local Gabor textons, Lecture Notes in Computer Science, in: Proceedings of the International Conference on Advances in Biometrics, Seoul, Korea, vol. 4642, 2007, pp. 49–57.
[40] S. Xie, S. Shan, X. Chen, X. Meng, W. Gao, Learned local Gabor patterns for face representation and recognition, Signal Processing 89 (2009) 2333–2344.
[41] H. V. Nguyen, L. Bai, L. Shen, Local Gabor binary pattern whitened PCA: a novel approach for face recognition from single image per person, in: Proceedings of the Third International Conference on Advances in Biometrics, Alghero, Italy, Lecture Notes in Computer Science, vol. 5558, 2009, pp. 269–278.
[42] A. Franco, D. Maio, D. Maltoni, 2D face recognition based on supervised subspace learning from 3D models, Pattern Recognition 41 (12) (2008) 3822–3833.
[43] J. Zou, Q. Ji, G. Nagy, A comparative study of local matching approach for face recognition, IEEE Transactions on Image Processing 16 (10) (2007) 2617–2628.

[44] T.K. Ho, J.J. Hull, S.N. Srihari, Decision combination in multiple classifier systems, IEEE Transactions on Pattern Analysis and Machine Intelligence 16 (1) (1994) 66–75.

[45] B. Gökberk, M. Okan Irfanoglu, L. Akarun, E. Alpaydin, Learning the best subset of local features for face recognition, Pattern Recognition 40 (5) (2007) 1520–1532.

[46] D. Goldberg, Genetic Algorithms in Search, Optimization & Machine Learning, Addison-Wesley, 1989.

[47] M. Mitchell, An Introduction to Genetic Algorithms, MIT Press, 1996.

[48] Á. Serrano, I.M. de Diego, C. Conde, E. Cabello, Recent advances in face biometrics with Gabor wavelets: a review, Pattern Recognition Letters . doi:10.1016/j.patrec.2009.11.002.

[49] J. Friedman, T. Hastie, R. Tibshirani, Additive logistic regression: a statistical view of boosting, Annals of Statistics 28(2) 337–374.

[50] J. Kittler, M. Hatef, R.P.W Duin, J. Matas, On combining classifiers, IEEE Transactions Pattern Analysis and Machine Intelligence 20 (3) (1998) 226–239.

[51] A.M. Martinez, R. Benavente, The AR Face Database, CVC Technical Report 24, 1998.

[52] A. Georghiades, P. Belhumeur, D. Kriegman, From few to many: illumination cone models for face recognition under variable lighting and pose, IEEE Transactions on Pattern Analysis and Machine Intelligence 23 (6) (2001) 643–660.

[53] K.-C. Lee, J. Ho, D. Kriegman, Acquiring linear subspaces for face recognition under variable lighting, IEEE Transactions on Pattern Analysis and Machine Intelligence 27 (5) (2005) 684–698.

[54] F. Samaria, A. Harter, Parameterization of a stochastic model for human face identification, in: Proceedings of the Second IEEE Workshop on Applications of Computer Vision, Sarasota, Florida, 1994, pp.138–142.

[55] C.E. Shannon, A mathematical theory of communication, The Bell System Technical Journal 27 (379-423) (1948) 623–656.

[56] T. Ahonen, A. Hadid, M. Pietikäinen, Face Recognition with local binary patterns, in: Proceedings Eighth European Conference on Computer Vision, 2004, pp. 469–481.

[57] X. Chai, S. Shan, X. Chen, W. Gao, Locally linear regression for pose-invariant face recognition, IEEE Transactions on Image Processing 16 (7) (2007) 1716–1725.

[58] A. Li,S. Shan, X. Chen, W. Gao, Maximizing intra-individual correlations for face recognition across pose differences, in: IEEE Conference on Computer Vision and Pattern Recognition CVPR 2009, Miami, FL, USA, 2009, pp. 605–611.

[59] A. Martin, G. Doddington, T. Kamm, M. Ordowski, M. Przybocki, The DET curve in assessment of detection performance, European Speech Processing Conference, Eurospeech 4 (1997) 1895–1898.

[60] W. Chen, M.J. Er, S. Wu, Illumination compensation and normalization for robust face recognition using discrete cosine transform in logarithm domain, IEEE Transactions on Systems, Man, and Cybernetics—Part B 36 (2006) 458–466.

[61] C.A. Perez, L.E. Castillo, L.A. Cament, P.A. Estevez, C.M. Held, Genetic optimization of illumination compensation methods in cascade for face recognition, Electronics Letters 46 (7) (2010) 498–500.

[62] Y. Guo, Z. Xu, Local Gabor phase difference pattern for face recognition, in: Proceedings of the 19th International Conference on Pattern Recognition (ICPR 2008), Tampa, FL, 2008, pp. 1–4.

[63] C. Xua, S. Lia, T. Tana, L. Quan, Automatic 3D face recognition from depth and intensity Gabor features, Pattern Recognition 42 (9) (2009) 1895–1905.

[64] M. Kirby, L. Sirvoich, Application of the Karhunen–Loeve procedure for the characterization of human faces, IEEE Transactions on Pattern Analysis and Machine Intelligence 12 (1990) 103–108.

Claudio A. Perez received the B.S. and P.E. in electrical engineering and the M.S. degree in biomedical engineering all from Universidad de Chile in 1980 and 1985, respectively. He was a Fulbright student at the Ohio State University where he obtained the Ph.D. in 1991. In 1990 he was a Presidential Fellow and received a Graduate Student Alumni Research Award from O.S.U. In 1991 he received a Fellowship for Chilean scientists from Fundacion Andes. He was a visiting scholar at UC, Berkeley in 2002 through the Alumni Initiatives Award Program from Fulbright Foundation. Currently he is a Faculty member at the Department of Electrical Engineering, University of Chile, where he was the chairman from 2003 to 2006. His research interests include human–machine interfaces, biometrics and pattern recognition. Dr. Perez is member of the editorial board of the International Journal of Optomechatronics and a Senior Member of the IEEE-SMC and IEEE-CIS, member of Sigma-Xi and OSU Alumni Association.

Leonardo A. Cament received the B.S. and P.E. in Electrical Engineering from Universidad de Chile in March 2008 with the highest honors. He is a Ph.D. student at the Department of Electrical Engineering, Universidad de Chile. His main interests in research are pattern recognition applied to eye detection, face recognition and human machine interfaces.

Luis E. Castillo received the B.S. and P.E. in Electrical Engineering from Universidad de Chile in December 2008. He is a Ph.D. student at the Department of Electrical Engineering, Universidad de Chile. His main interests are pattern recognition applied to face recognition and illumination compensation.